Title

Patchiness of plankton communities at fronts explained by Lagrangian history of upwelled water parcels

Journal

Limnology and Oceanography, 69(9)

ISSN

0024-3590 1939-5590

Authors

Gangrade, Shailja

Mangolte, Inès

Publication Date

2024-08-12

DOI

10.1002/lno.12654

Data Availability

The data associated with this publication are available at: https://oceaninformatics.ucsd.edu/datazoo/catalogs/ccelter/datasets

Peer reviewed

LIMNOLOGY and OCEANOGRAPHY

ASLO

Limnol. Oceanogr. 69, 2024, 2123–2137

doi: 10.1002/lno.12654

Patchiness of plankton communities at fronts explained by Lagrangian history of upwelled water parcels

Shailja Gangrade [1*] **Inès Mangolte** [2,3]

[1]Scripps Institution of Oceanography, University of California San Diego, La Jolla, California, USA
[2]LOCEAN (Laboratoire d'Océanographie et du Climat), Institut Pierre Simon Laplace (Sorbonne Université/CNRS/IRD/MNHN), Paris, France
[3]ENTROPIE, IRD/Université de la Réunion/Université de Nouvelle-Calédonie/CNRS/Ifremer, Noumea, New Caledonia

Abstract

The transport of plankton by highly dynamic (sub)mesoscale currents—often associated with fronts and eddies—shapes the structure of plankton communities on the same time scales as biotic processes, such as growth and predation (days–weeks). The resulting biophysical couplings generate heterogeneities in their finescale distributions (1–10 km), or "patchiness." Here, we test the hypothesis that cross-frontal plankton patchiness at a front found 200–250 km offshore in the California Current System was influenced by wind-driven upwelling conditions upstream of the front. We show that in situ Eulerian measurements (cross-frontal transects) can be interpreted in a Lagrangian framework by using satellite-derived current velocities to trace water parcels backward in time to their coastal origins. We find that the majority of the water parcels sampled at this front originated along the central California coast during different episodic wind-driven upwelling pulses and followed various trajectories before converging temporarily at the front. In response to nutrient injections at the coast, plankton communities transformed during their journeys from the coast to the sampling zone, with a succession of phytoplankton and zooplankton blooms. The cross-frontal sampling captured the convergence of these distinct water parcels at different points in their biological histories, which resulted in the observed spatial patchiness. Our results suggest that identifying the processes controlling frontal plankton communities requires understanding them in the context of their spatial and temporal histories. In particular, Lagrangian approaches should be more widely applied to understand critical ecological patterns in highly dynamic systems.

Marine plankton are passively drifting organisms of immense ecological and biogeochemical importance in the functioning of ocean ecosystems. Plankton spatial distributions are profoundly impacted by ocean currents, particularly in regions of highly energetic mesoscale stirring. In stirring features, such as fronts and eddies, horizontal current velocities can reach up to 50–80 km d^{-1} (Barth et al. 2000; McWilliams 2016; Zaba et al. 2021), resulting in transport over long distances within a few days to weeks. Importantly, biological processes, such as growth, competition, or predation, occur on similar time scales. Phytoplankton blooms, for instance, can develop within a few days given adequate light and nutrient availability, such as during spring blooms (Lewandowska et al. 2015) or in upwelling filaments (Zaba et al. 2021). Most mesozooplankton can complete a reproduction cycle in a few weeks (Eiane and Ohman 2004; Deibel and Lowen 2012).

As a result, physical and biological processes are highly coupled, often resulting in a high level of heterogeneity in biological properties on small spatial scales (1–10 km), or "patchiness." Disentangling the interacting roles of physics and biology in driving plankton patchiness has been a central question in ecology for many decades (Levin and Segel 1976; Martin 2003; McGillicuddy and Franks 2019). The processes driving plankton diversity and community structure have similarly been examined, with many studies showing the influence of

*Correspondence: sgangrad@ucsd.edu

Additional Supporting Information may be found in the online version of this article.

Author Contribution Statement: SG: Conceptualization (equal); Data curation (equal); Formal analysis (lead); Methodology (equal); Software (lead); Visualization (lead); Writing – original draft preparation (equal); Writing – review and editing (equal). IM: Conceptualization (equal); Data curation (equal); Formal analysis (supporting); Software (supporting); Visualization (supporting); Methodology (equal); Writing – original draft preparation (equal); Writing – review and editing (equal).

bottom-up and top-down trophic interactions (Allen et al. 2005; Dugenne et al. 2020; Mangolte et al. 2022), transport (Wilkins et al. 2013), or a combination of all of these processes (Clayton et al. 2013; Schmid et al. 2023). Lagrangian studies have also explored how water parcels are connected between remote regions (i.e., their "connectivity") across differing spatial scales—from a single basin to the global ocean—and how this connectivity influences various biological processes, such as genetic similarity or larval dispersal (Wilkins et al. 2013; Rossi et al. 2014; Jönsson and Watson 2016).

Recently, many studies have employed Lagrangian approaches to describe how plankton communities transform as they are transported, sometimes hundreds of kilometers in a matter of days (Messié and Chavez 2017; Lehahn et al. 2018; Messié et al. 2022). These approaches have shown that the abundance of plankton is not only determined by their immediate environment (e.g., temperature and nutrient concentration; Mousing et al. 2016; Tzortzis et al. 2021; Haberlin et al. 2019), but is also shaped by the conditions experienced during the previous weeks at different locations (d'Ovidio et al. 2010; Gangrade and Franks 2023; Hernández-Carrasco et al. 2023). The first view—local environmental conditions determine species abundance—can be likened to the classic Eulerian concept of an "ecological niche." This concept was originally developed for terrestrial ecosystems and successfully applied to the ocean on large scales (e.g., biogeochemical provinces as in Longhurst (2006)). The second view—transport history shapes species distributions—is a Lagrangian concept, relevant to small scales and specific to passively drifting marine plankton. This concept has been described as "fluid dynamical niches" (d'Ovidio et al. 2010): finescale plankton patchiness is a moving mosaic of water parcels carrying different plankton communities.

Here, we investigate the processes generating finescale cross-frontal patchiness in plankton community structure in an upwelling system, the California Current System (CCS). In an Eastern Boundary Upwelling System (EBUS) such as the CCS, wind-driven vertical nutrient injections at the coast modulate biological variability at time scales ranging from days to decades (Jacox et al. 2018; Messié et al. 2023), while horizontal currents structure the ecosystem spatially by advecting recently upwelled waters in filaments from the coast to offshore (Chelton et al. 2011; Rossi et al. 2013; Zaba et al. 2021). The California Current System is thus structured by a cross-shore gradient: new production (primary production resulting from nutrient inputs from outside the euphotic zone, such as coastal upwelling) generally takes place inshore while export takes place further offshore (Stukel et al. 2013; Chabert et al. 2021). In addition to the small-scale circulation (filaments and eddies), the California Current System is composed of two main flow features: the California Current (CC), an equatorward-flowing current of subarctic origin, and the California Undercurrent (CU), a subsurface poleward-flowing current of equatorial origin (Lynn and Simpson 1987; Bograd et al. 2019).

We use the case study of a front in the southern California Current System, characterized by an intense frontal jet and horizontally converging flow (de Verneil et al. 2019), to explore how coastal upwelling pulses propagate offshore (Gangrade and Franks 2023) and generate plankton patchiness (Mangolte et al. 2023) on time scales of a few weeks. We evaluate the relationship between plankton distributions and the characteristics of water parcels based on two different frameworks. First, we describe the water parcels by their in situ hydrographic properties (the *regional water-mass types* derived from temperature and salinity: CC or CU). Second, we describe the water parcels based on their Lagrangian trajectories since upwelling (the *water-mass history*, derived from a backtracking analysis). Our results show that both frameworks give insights into the drivers of plankton community structure; however, the Lagrangian method provides a more detailed understanding of the mechanisms generating local finescale patchiness.

Data and methods

Cruise data

Biological and hydrographic measurements were collected during the California Current Ecosystem Long-Term Ecological Research (CCE LTER) Process Cruise P1208 in August 2012. This cruise sampled an eddy-associated front, dubbed "E-Front," located approximately 200–250 km offshore of Point Conception, California. This front was positioned between an anticyclonic eddy to the west (offshore) and a cyclonic eddy to the east (inshore) (de Verneil and Franks 2015; Stukel et al. 2017). The cross-frontal sampling included two transects (E1 and E2) with high horizontal resolution (3–5 km between consecutive stations), conducted on August 4–5, 2012 and August 20–21, 2012, respectively (Fig. 1).

At each transect station, a CTD (conductivity, temperature, depth) vertical profile was recorded down to 350 m and binned to 1-m vertical resolution, and water samples were collected in Niskin bottles at discrete depths (5–6 levels between 0 and 100 m) on the ascent. The CTD rosette included a fluorometer which measured in vivo chlorophyll *a* (Chl *a*) fluorescence. After the CTD cast, zooplankton samples were collected with a 0.71-m diameter, 202-μm mesh vertical Bongo net tow from 0 to 100 m. The plankton samples were later analyzed using three different methods; the full dataset was described in detail in Mangolte et al. (2023) (*see* their Fig. 2) and is summarized here (Supporting Information Table S1). Flow cytometry was performed on the Niskin bottle water samples (0–100 m), producing the abundance (number of cells L^{-1}) of four taxa of pico-plankton (< 2 μm) identified by their light-scattering properties. High-performance liquid chromatography (HPLC) was performed on the surface Niskin bottle samples; the concentrations of Chl *a* and accessory pigments

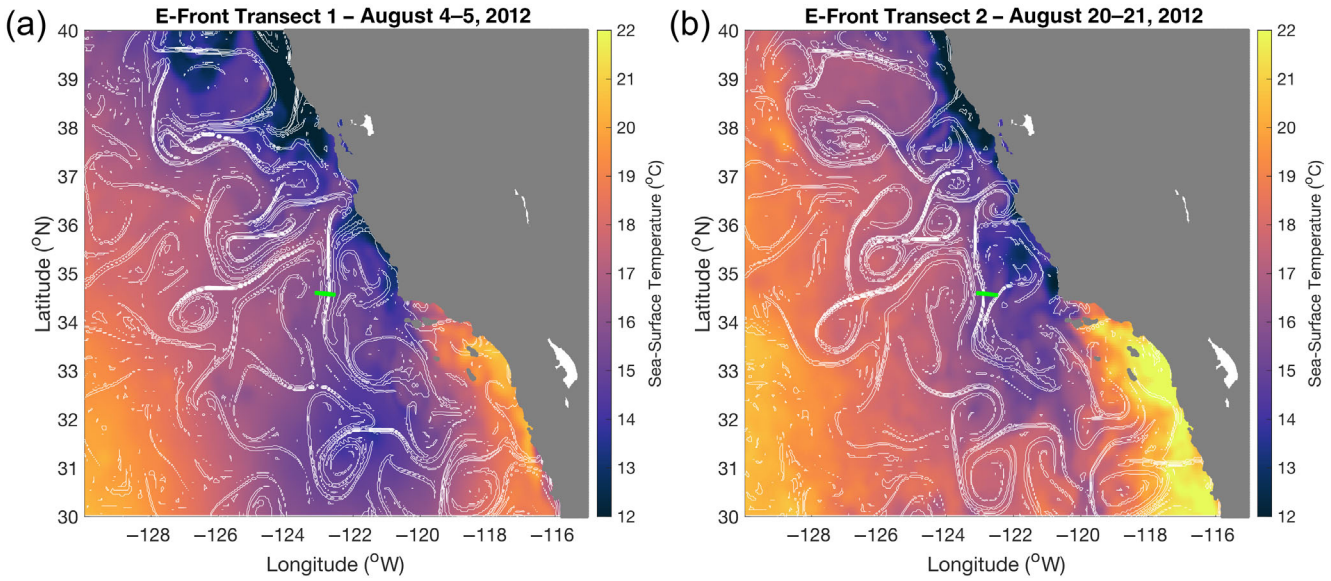

Fig. 1. Maps of sea-surface temperature (SST in °C, color scale) and finite size Lyapunov exponents (FSLEs in d^{-1}, white contours) averaged over the duration of E-Front Transect E1 (**a**) and Transect E2 (**b**). We used FSLEs to visualize the transport patterns creating convergent flow structures such as fronts. FSLE contours represent values from 0 to -0.3 d^{-1}, in increments of 0.1 d^{-1}. Green markers indicate the locations of the sampling stations in each transect. Filaments of recently upwelled cold water were advected offshore via mesoscale stirring features (outlined by the FSLE contours) at various locations along the coast (e.g., at 38°N in Transect E2).

were measured and used to determine the contributions (percentage) of eight phytoplankton taxa relative to the total chlorophyll (Goericke and Montoya 1998). Zooplankton samples, collected from vertical Bongo nets, were preserved in 1.8% buffered formaldehyde, and organisms were then identified in the lab using the ZooScan semi-automated imaging system (Ohman et al. 2012) with 100% manual validation, producing the vertically integrated abundance (number of organisms m^{-2}) of 15 groups of mesozooplankton.

Water-mass classification

We classified the waters sampled by the CTD as California Current (CC) or California Undercurrent (CU) based on their salinity and temperature values. We used criteria that were defined by Zaba et al. (2021) using climatological measurements from the California Underwater Glider Network. They first identified the currents by their velocities (poleward for the CU vs. equatorward for the CC) and then determined the corresponding boundaries in temperature–salinity space. Thus, waters saltier and warmer than the CU threshold were classified as CU, while waters fresher and colder than the CC threshold were classified as CC. Waters with intermediate salinity and temperature values were assumed to be composed of a mixture of CC and CU water and were classified as MIX (Supporting Information Fig. S1).

Statistical analysis of water-mass type and abundance association

We combined the information on hydrographic classifications (CC, CU, or MIX) and plankton abundances to determine whether plankton were preferentially associated with a certain water mass. For phytoplankton and bacteria, we used abundances and water-mass type classification at each Niskin bottle depth. Because the Bongo nets generate vertically integrated zooplankton abundances, we found it most informative to relate the zooplankton distributions to the dominant water-mass type in the sampled water column (0–100 m). We defined this dominant water type as CC or CU if more than 50% of the vertical bins were classified as such, and MIX in other cases. The abundances of bacteria, phytoplankton, and zooplankton in each water-mass type were first examined qualitatively (Supporting Information Figs. S2–S5) and Kruskal–Wallis tests were then used to determine whether abundances among the three water-mass types were statistically different.

Water-parcel tracking

We advected the water parcels backward in time from initial locations (i.e., each transect station), using the following equations:

$$x(t+\Delta t) = x(t) + u(x,y,t) \times \Delta t, \quad (1)$$

$$y(t+\Delta t) = y(t) + v(x,y,t) \times \Delta t. \quad (2)$$

Instead of a positive Δt, we applied a $\Delta t = -1$ d and iteratively computed x and y for the 2 months (66 d) preceding the transect date. We limited the backtracking to 2 months because the contribution of stirring and mixing to water-mass property changes is likely to be smaller than the contribution

of advection for this duration. We used a 2D advection scheme with surface velocities because upwelled waters parcels are likely to stay near the surface for this duration. We used the "GLOBCURRENT" velocity product from the Copernicus Marine Environment Monitoring Service (CMEMS; https://doi.org/10.48670/mds-00327), which consists of surface zonal and meridional velocities ($u(x,y,t)$, $v(x,y,t)$) with a 1-d temporal resolution and a 0.25° horizontal resolution. When water-parcel locations (x,y) fell between grid points, we linearly interpolated the GLOBCURRENT gridded velocity product to obtain ($u(x,y,t)$, $v(x,y,t)$) at each location along the trajectory. The velocities include a geostrophic component (derived from satellite altimeter measurements) and a wind-driven Ekman component at 0 m and 15 m depth, derived from the wind stress from the ERA reanalysis (Rio et al. 2014). We selected the 15-m Ekman component because it is more representative of the movement of the euphotic layer, which was measured to be 60–70 m during this same cruise (Stukel et al. 2017), than the 0-m component. Additionally, we used backward-in-time finite-size Lyapunov exponents (FSLEs) to visualize transport patterns creating convergent flow structures such as fronts. The FSLEs represent the exponential rate of separation (when calculated forward-in-time) or convergence (when calculated backward-in-time) of water-parcel trajectories. The FSLEs, obtained from Aviso + (https://doi.org/10.24400/527896/a01-2022.002), were calculated with a final separation distance of 0.6° and advected by altimetry-derived velocities (d'Ovidio et al. 2004).

Random parcel seeding

To estimate the uncertainty associated with these trajectories (primarily caused by the coarse 0.25° spatial resolution of the velocities, representing approximately two velocity data points in each 50 km transect), we performed the backtracking for 100 parcels seeded randomly within a 0.0625° (approximately 5 km) radius around each transect station. The distance between stations ranged between 1 and 10 km, with an average of about 5 km. We then described the presumed upwelling conditions experienced by the waters sampled at each station based on this ensemble of possible trajectories.

Upwelling pulses

Wind-driven upwelling pulses were determined from the Coastal Upwelling Transport Index (CUTI; Jacox et al. 2018), which is defined in 1° latitudinal bands. We defined anomalies relative to the temporal average of the CUTI during the study period (June to August 2012). Upwelling pulses were defined as short periods (typically a few days) of positive CUTI anomalies. Large positive anomaly values indicate strong upwelling pulses that are expected to upwell high-nutrient waters from below the euphotic zone and generate a strong biological response.

Upwelling conditions upstream of the front

We used the backward-in-time trajectories and Coastal Upwelling Transport Index (CUTI) values along the California coast to determine how many days before being sampled at the front a water parcel had experienced an upwelling pulse, and the intensity of that pulse. First, we determined whether each sampled water parcel was in the coastal region influenced by wind-driven upwelling (i.e., within 25 km of the coastline; Huyer 1983) in the 2 months before sampling. Next, for parcels with coastal origins, we determined whether the parcel experienced an upwelling pulse. If it did, we recorded the location (latitude, longitude, and date) of the water parcel when it was last at the coast during an upwelling pulse; these coordinates thus represented the parcel's temporal and spatial origin. Finally, we characterized a parcel's upwelling pulse using two criteria: (1) the intensity of the upwelling pulse (Coastal Upwelling Transport Index anomaly) at the parcel's origin and (2) the water parcel age since the upwelling pulse (i.e., the time elapsed between the origin date and the frontal sampling date, in days). We followed this procedure for all 100 points seeded around each transect station.

Results

Distribution of water masses and Chl *a* across the front

In the upper 100 m, the eastern (inshore) side of the front was composed of primarily CU waters while the western (offshore) side was composed of primarily CC waters (Fig. 2). The interface between the water masses, where water-mass mixing occurred, was composed of a 2–15 km wide layer of MIX waters. While this MIX layer persisted for at least the duration of the cruise (approximately 1 month), its geometry changed between the two transects, which were sampled 2 weeks apart. During the first transect (E1, Fig. 2a), the MIX water layer between the CC and CU water masses was tilted across the front, with CU waters extending offshore below the CC waters (and vice versa: CC waters extending inshore above CU waters). During the second transect (E2, Fig. 2b), the MIX layer was mostly vertical, with the exception of an intrusion of offshore CC waters into inshore CU waters below the surface (30–70 m).

The distribution of Chl a fluorescence (Fig. 2, hatched contours) across the front was closely related to the distribution of the water masses. Generally, CC waters contained less Chl a than CU waters. Most strikingly, small patches of high Chl a were associated with MIX waters at the interface between CC and CU waters. This visual pattern was then confirmed by the results of a Kruskal–Wallis statistical test summarized in Table 1, where statistically significant associations are indicated by "X," and taxa with a weak association with a water mass (identified qualitatively, but without passing the Kruskal–Wallis tests) with "x." The geometry of the Chl a patches was closely aligned with the boundaries between the water masses, consistent with a coupling of hydrographic and

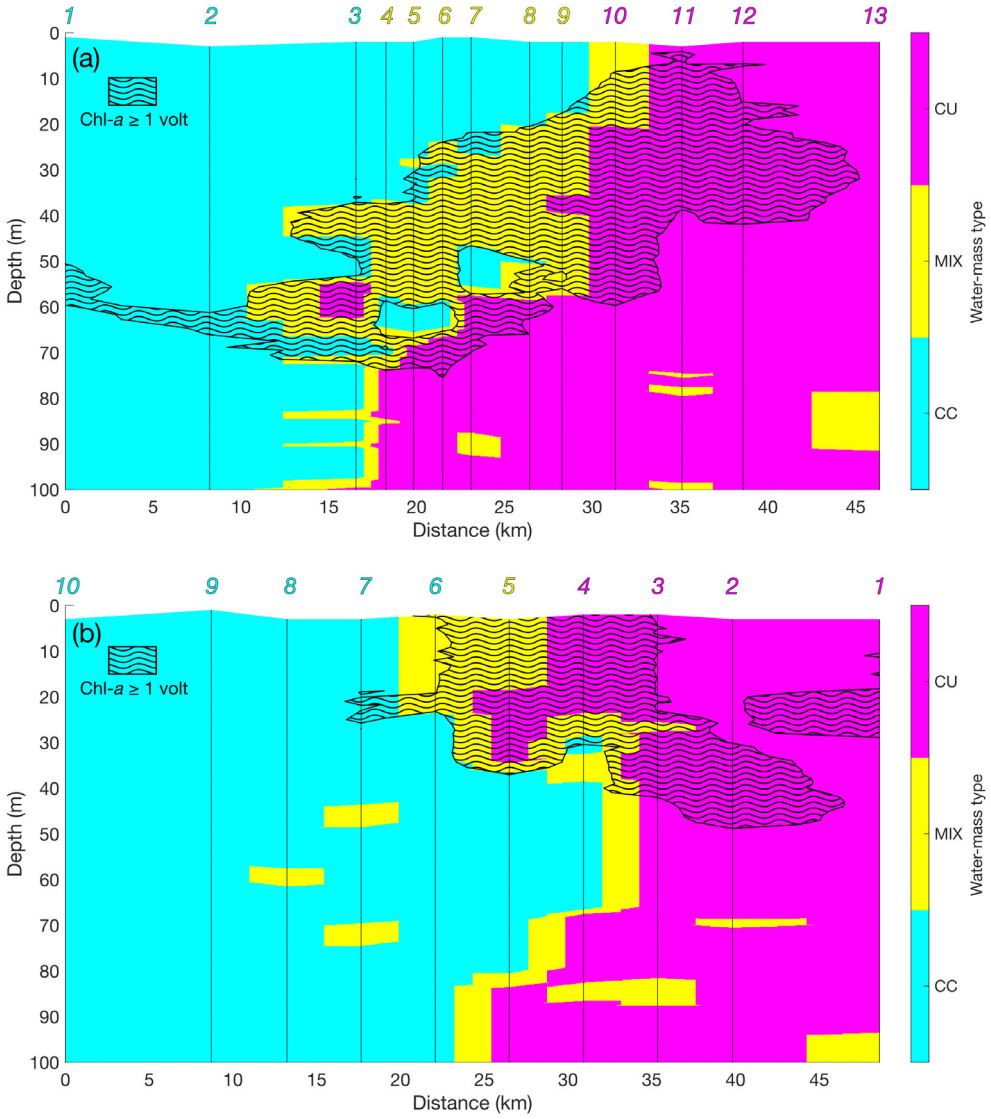

Fig. 2. Vertical sections (0–100 m) across the front from west (offshore, on the left) to east (inshore, on the right) of water masses for Transect E1 (**a**) and Transect E2 (**b**). Cyan, magenta, and yellow colors indicate California Current (CC), California Undercurrent (CU), and Mixed (MIX) waters, respectively. Here, the frontal interface coincided with the MIX waters (yellow). Hatches show the position of chlorophyll *a* patches (fluorescence ≥ 1 *V*). Vertical black lines indicate the position of the CTD stations, with the station number colored by the majority water-mass type on the top *x*-axis.

biological properties. In the next section, we investigate this coupling in more detail by looking at the individual phytoplankton and zooplankton taxa.

Distribution of plankton taxa across the front

We analyzed the spatial distribution of 23 plankton taxa (including bacteria, phytoplankton, and zooplankton) across the front to characterize their relationship with water-mass type. We found that spatial distribution across the front varied by taxon; bacteria, phytoplankton, and zooplankton were not necessarily co-located in space in terms of abundance (Fig. 3). This cross-frontal patchiness and variability both within and across transects prompted us to investigate the association of each taxon with water-mass type.

We considered that a given taxon was consistently associated with CC or CU if it had a significantly higher abundance in that water-mass type for the two transects conducted 2 weeks apart during the cruise. We found that eight taxa (chlorophytes, cryptophytes, dinoflagellates, pelagophytes, prymnesiophytes, heterotrophic bacteria, rhizaria, and pteropods) were consistently associated with CU waters, and one taxon (*Prochlorococcus*) was consistently associated with CC waters in both transects (Table 1, upper rows).

The remaining taxa ($n = 14$) did not have a consistent association with a single water-mass type (CC or CU) and displayed a range of patterns (Table 1, bottom rows). Ostracods were associated with MIX waters in both transects, while the 13 other taxa exhibited time-dependent water-mass associations.

Table 1. Association between plankton taxa and water-mass types. Different market indicate different associations: X = statistically significant association; x = minor association; — = no association. The upper rows (Chlorophytes to *Prochlorococcus*) indicate taxa that were consistently associated with a single water-mass type (CC or CU), while the bottom rows (Chlorophyll *a* fluorescence to Other crustaceans) indicate taxa that were not consistently associated with a single water-mass type. The full results of the Kruskal–Wallis tests are provided in Supporting Information Tables S2 and S3.

	CC		MIX		CU	
Taxa	***E*1**	***E*2**	***E*1**	***E*2**	***E*1**	***E*2**
Chlorophytes	—	—	—	—	X	X
Cryptophytes	—	—	—	—	X	X
Dinoflagellates	—	—	—	—	X	x
Pelagophytes	—	—	—	—	X	x
Prymnnesiophytes	—	—	—	—	X	x
Heterotrophic bacteria	—	—	—	—	X	X
Rhizaria	—	—	—	—	x	X
Pteropods	—	—	—	—	X	X
Prochlorococcus	X	X	—	—	—	—
Chlorophyll *a* fluorescence (0–100 m)	—	—	X	X	—	—
Ostracods	—	—	x	x	—	—
Diatoms	—	—	—	x	—	—
Synechococcus	—	—	X	—	—	—
Pico-eukaryotes	—	—	X	—	—	—
Appendicularians	—	—	x	—	—	—
Chaetognaths	—	—	x	—	—	—
Cnidarians	—	—	x	—	—	—
Doliolids	—	X	—	—	x	—
Copepods (Calanoids, Oithona, others)	—	—	x	—	—	x
Polychaetes	—	—	X	—	—	x
Euphausiids	—	—	x	—	—	x
Other crustaceans	—	—	x	—	—	x

CC, California Current; CU, California Undercurrent; MIX, Mixed.

Doliolids were associated with CU waters in E1, but CC waters in E2; three copepod taxa, polychaetes, euphausiids, and other crustaceans were associated with MIX waters in E1, but with CU waters in E2. The remaining taxa were associated with a particular water mass in only one transect, with no statistically significant association in the other: pico-eukaryotes, *Synechococcus*, chaetognaths, cnidarians, and appendicularians were associated with MIX waters in E1 only; diatoms were associated with MIX waters in E2 only (Supporting Information Tables S2, S3).

While the distributions of some plankton taxa were explained by the local water-mass type (consistent association with either CC or CU), the majority were not. In the next sections, we explore the possibility that the water-mass history (through a Lagrangian approach) could provide an alternative explanation.

Horizontal convergence of water masses at the front

Here, we examine the origins of the water parcels sampled across the front to investigate how wind-driven coastal upwelling upstream of the front drove temporal and spatial biological variability across the front.

Geographic origins

Our backward-in-time tracking showed that waters sampled during both E1 and E2 had variable geographic origins (Fig. 4). While almost all the stations contained waters that originated at the coast in the 2 months before sampling (Supporting Information Table S4), the origin locations varied. Waters sampled in E1 originated from a broad stretch of the coast (from 34°N to 39°N, about 500 km), while the waters sampled in E2 originated in a narrower region (34°N to 36°N, about 200 km). Thus, for both transects, water parcels sampled within 25 km of each other at the front were hundreds of kilometers apart 2 months earlier. The lengths and geometries of parcel trajectories from the coast to the transect locations were also variable: water parcels sampled on the offshore side of the transects generally had long, meandering trajectories, while water parcels sampled on the inshore side of the transects generally had shorter, more direct trajectories to the front (Fig. 4).

Temporal origins: Upwelling pulses

Water parcels sampled at the frontal transect sites also originated at the coast at different times. For simplicity, we assumed that water parcels originating in the coastal region during an upwelling pulse were upwelled from depth. Remarkably, despite the fact that upwelling pulses only occurred 40–50% of the time (Fig. 5), our backtracking analysis revealed that almost all the water parcels sampled during the cruise originated at the coast during an upwelling pulse (Supporting Information Table S4). Some of the sampled parcels were upwelled much more recently than others: the median ages (times since upwelling) ranged from 8 to 51 d for Transect E1, and from 11 to 43 d for Transect E2 (Fig. 6). For E1, the inshore stations tended to contain more recently upwelled water than the offshore stations (Fig. 6a). However, counter-intuitively, for E2, the oldest waters (median age = 43 d) were found at the two most inshore stations (E2 Stas. 1 and 2), while the other stations contained more recently upwelled water with median ages ranging from 11 to 15 d (Fig. 6b). We discuss this apparent discrepancy further in the next section. Finally, we found that the intensities of the upwelling pulses were variable along the coast, with the Coastal Upwelling Transport Index anomaly ranging from approximately 0 to 1.8 m^2s^{-1}(Figs. 5, 6).

Relationship between upwelling and water masses

The distributions of CC and CU waters across the front were related to their geographic and temporal origins during upwelling pulses. The data collected during the Transect E1 supported the typical scenario of subsurface nearshore CU waters being entrained first upward (into the euphotic zone by upwelling) and then offshore by transport (Zaba

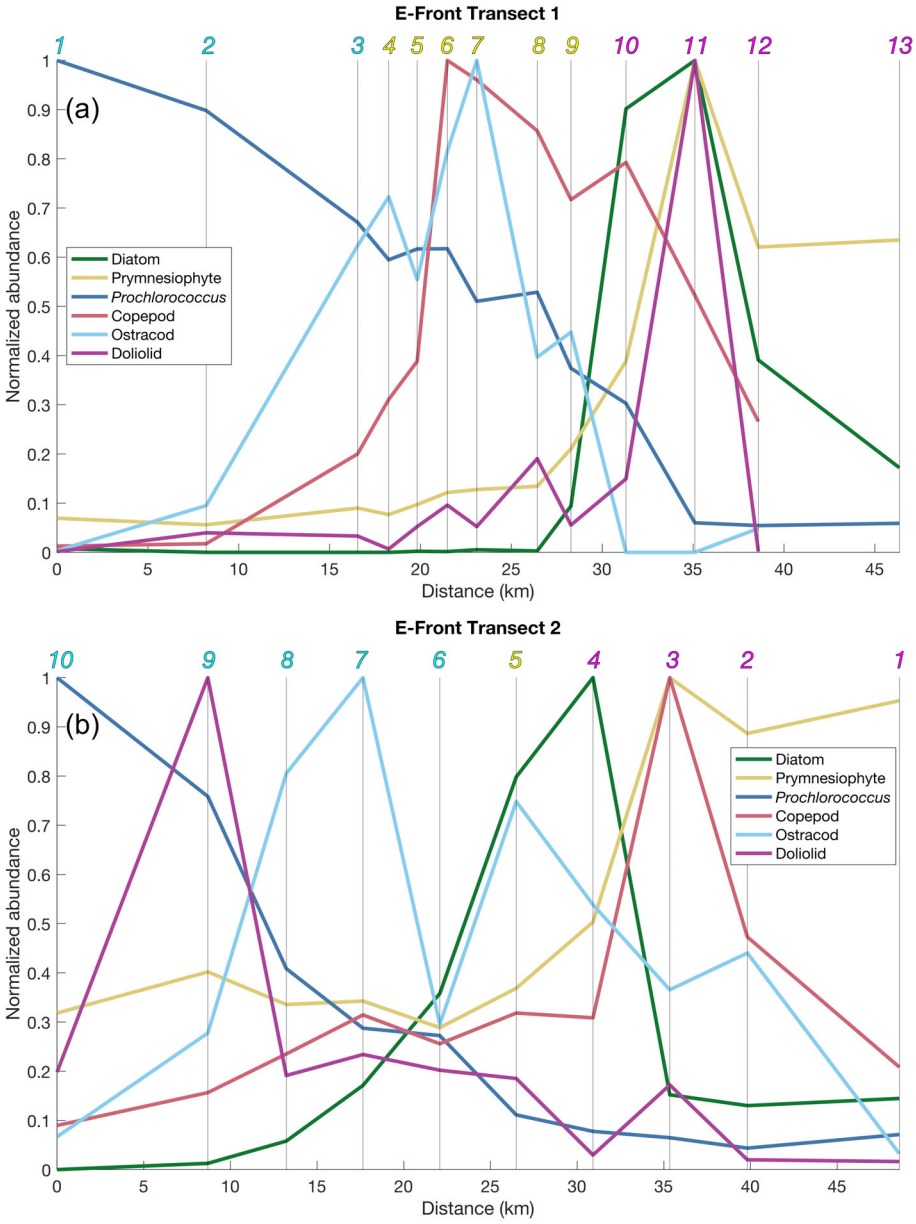

Fig. 3. Cross-frontal abundances, normalized by the maximum abundance for each taxon in each transect, of select bacteria, phytoplankton, and zooplankton taxa in Transect E1 (**a**) and Transect E2 (**b**). Top *x*-axis and vertical black lines indicate locations of the stations for each transect, and coloring of transect station numbers correspond to water-mass type as defined in Fig. 2 (cyan for California Current [CC], magenta for California Undercurrent [CU], and yellow for Mixed [MIX]). The color of each plotted line represents a specific taxon.

et al. 2018). The water parcels with short, direct trajectories between coastal upwelling sites and the transect location (E1 Stas. 10–13) retained a CU temperature-salinity signature, while parcels with long, meandering, offshore trajectories (E1 Stas. 1–9) mixed with CC waters, leading to their classification as MIX, and CC for the oldest water parcels (Figs. 2, 4).

Data from E2, however, indicate a more complicated scenario. E2 included recently upwelled water parcels (with very short and direct trajectories from the coast) that were classified as CC (E2 Stats. 5–10). Conversely, some older water parcels with long meandering trajectories were classified as CU (E2 Stats. 1–2, Figs. 4, 6). Some trajectories can be seen meandering strongly between offshore and coastal regions (Fig. 4); this suggests that CC waters may have first been brought from offshore into the coastal regions and then were advected offshore again along with newly upwelled waters.

Biological history along water-parcel trajectories

We investigated the relationship between the age of an upwelled water parcel and the plankton community found

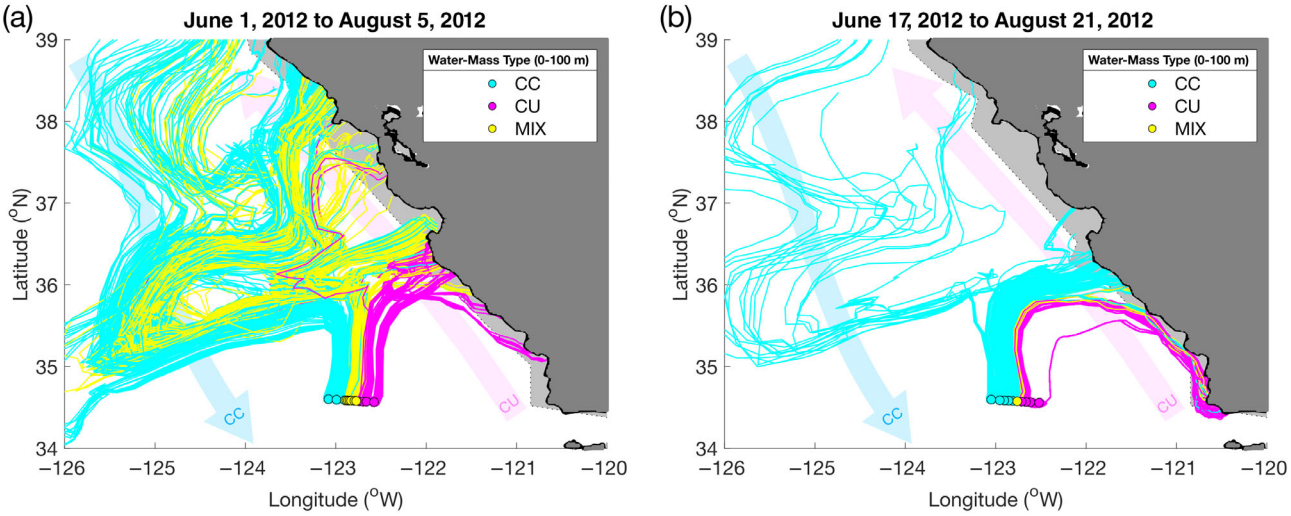

Fig. 4. Trajectories of water parcels sampled across E-Front Transect E1 (**a**) and Transect E2 (**b**) in the 2 months before sampling. Trajectories were computed from backward-in-time advection, using a velocity field that includes a geostrophic and a 15-m depth Ekman component. Filled circles show the locations of the sampled stations, with each station consisting of a CTD (conductivity, temperature, depth) cast and a Bongo net tow. For each station, the back-trajectories of 100 points, randomly seeded in a 5-km radius around the actual station, were computed. The colors of each circle and trajectory pathline correspond to the dominant water-mass type of the water parcel when it was sampled (as defined in Fig. 1). The light gray region outlined by the dotted line indicates the coastal upwelling region, which encompasses the coastal region within approximately 25 km of the coastline. The blue and magenta arrows show the approximate position and direction of the California Current [CC] and California Undercurrent [CU], respectively.

within this water parcel. We defined the "biological history" of a water parcel as the relationship between its age (defined as time since upwelling) and abundances of key planktonic taxa within that water parcel. By combining the trajectories of water parcels of different ages, we reconstructed the biological histories of these water parcels between the upwelling pulse (at the coast) and sampling (at the transects). Since we found no relationship between plankton abundance and upwelling pulse intensity (Supporting Information Figs. S6–S8), we assumed that all upwelling pulses generated a similar biological response.

We found that the abundances of diatoms and copepods exhibited the clearest relationship with age since upwelling, with peaks at about 15 and 30 d, respectively, after a water parcel experienced an upwelling pulse (Fig. 7). This succession is consistent with the well-known trophic dynamics of these two taxa. In this region, diatom doubling times are only a few days under nutrient-rich conditions (Sarthou et al. 2005),

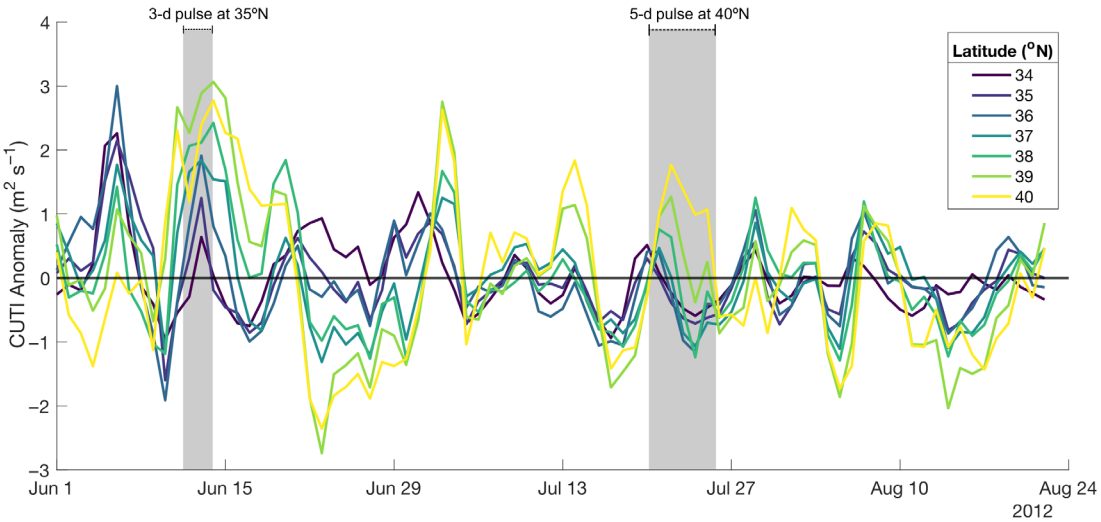

Fig. 5. Times series of the Coastal Upwelling Transport Index (CUTI) anomaly from June 1, 2012 to August 24, 2012 for different latitudinal bands (colors) in the California Current System. Two contrasting upwelling pulses are highlighted (gray-shaded regions), illustrating upwelling variability in terms of location, timing, duration, and intensity.

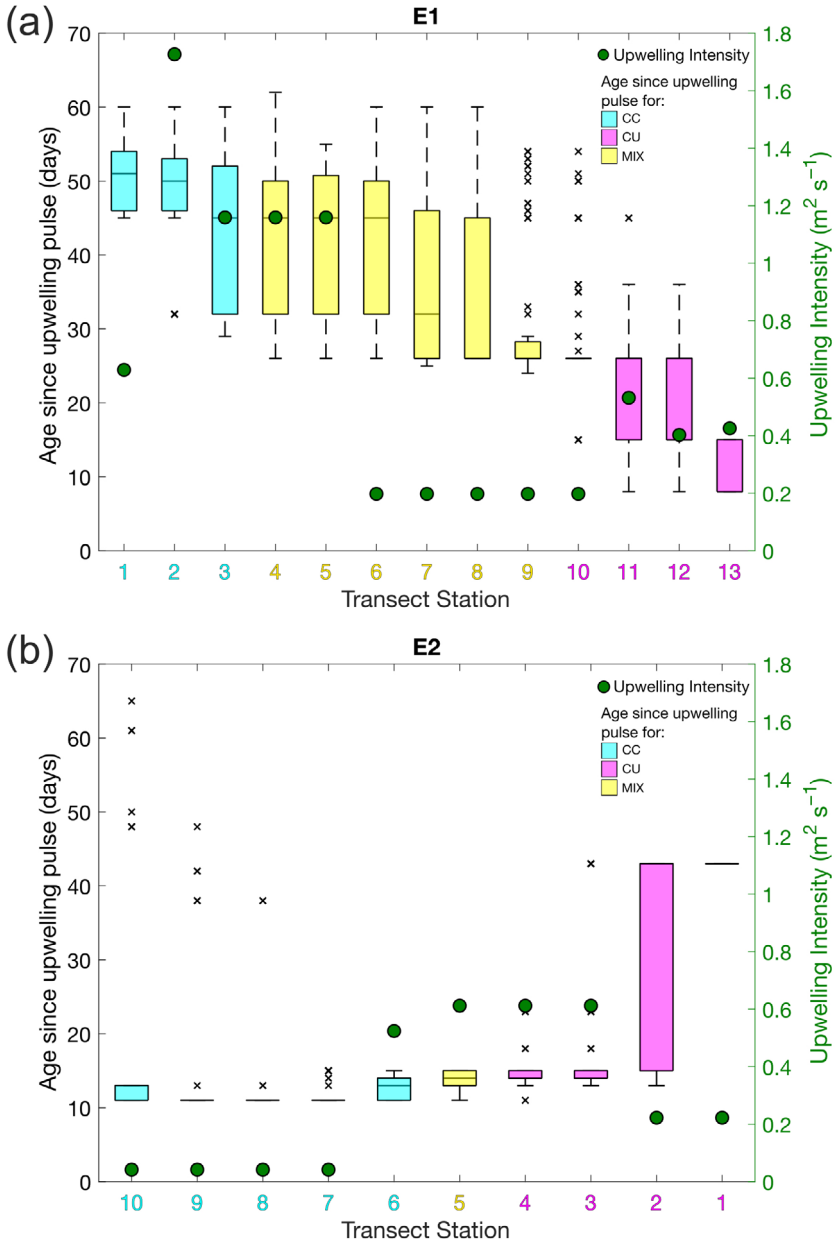

Fig. 6. Upwelling conditions experienced by the ensemble of trajectories for each sampled station of Transect E1 (**a**) and Transect E2 (**b**). Box plots show the interquartile range of age since upwelling pulse in days (left *y*-axis, with outliers indicated by black *x*-markers). Box plots and transect station numbers are colored by the majority water-mass type at each station. Green filled circles indicate the median upwelling intensity, calculated as the Coastal Upwelling Transport Index (CUTI) anomaly, when parcels were at the coast (right *y*-axis in green).

though times may vary depending on the exact nutrient and diatom species present. Copepods, which are among the main predators of diatoms, can complete a reproduction cycle in 28 d (Eiane and Ohman 2004). Thus, we interpreted this succession of abundance peaks as a diatom bloom in response to the upwelling pulse, followed by a copepod bloom in response to the increase of their food supply. The other taxa showed more complex relationships between abundance and age, which, due to higher uncertainties regarding their food-web dynamics and growth rates, prevented us from deriving robust interpretations of the influence of the upwelling pulses (*see* Supporting Information "Biological responses of non-diatom and non-copepod taxa" section and Figs. S6–S8).

Discussion

In this study, we sought to investigate the influence of wind-driven coastal upwelling on the finescale plankton community structure observed across a front. We first attempted to relate the ecosystem structure to the hydrographic

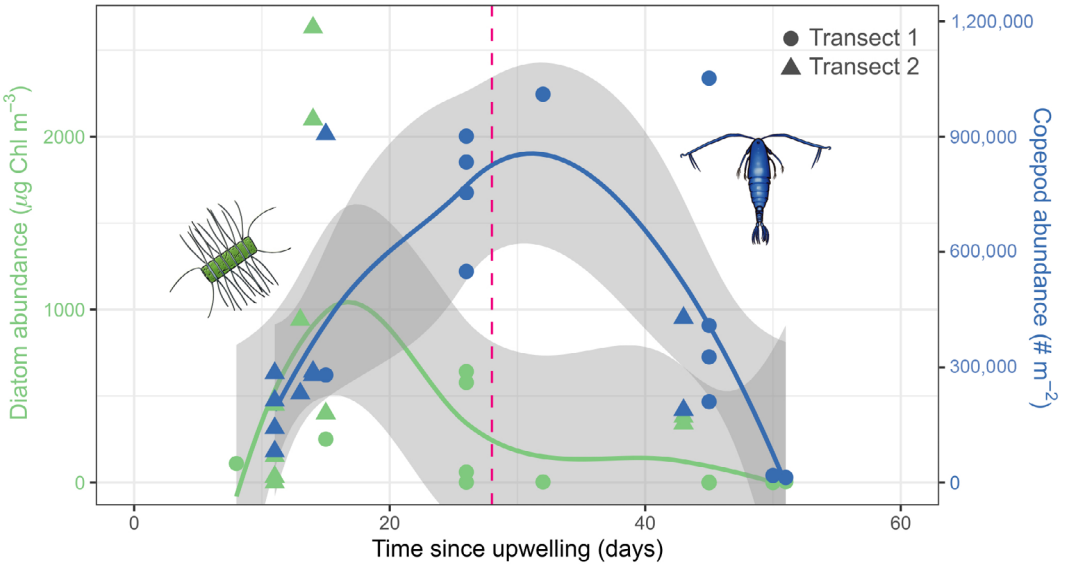

Fig. 7. Relationship between plankton abundance and time since upwelling for diatoms (prey) in green and copepods (predator) in blue. Each marker represents one station (triangles for Transect E1, circles for Transect E2). The green and blue lines represent the locally weighted scatterplot smoothing (LOWESS) fits ($f = 0.75$) for the diatom and copepod abundances respectively. The gray shaded regions indicate the 95% confidence interval for each LOWESS fit. The vertical dashed line in magenta indicates the typical copepod generation time (28 d). Plankton illustrations: Freya Hammar.

properties of water (the water-mass type, CC or CU), relying on previous literature that established that CU waters are generally recently upwelled while CC waters are found offshore. However, we found that the explanatory power of this approach was limited: many plankton taxa were either found at the interface between the two water masses, or they did not have a consistent association with a particular water-mass type.

We then used a Lagrangian approach to describe the history of the water parcels by backtracking each parcel to its origin. Our results from this approach demonstrated a consistent story (Fig. 8). Intermittent increases in alongshore wind generated short upwelling pulses every week or so, transporting deep, nutrient-rich waters into the euphotic zone in the coastal region. These water parcels were then advected offshore, following distinct trajectories until they reached the front where they were sampled. During this advection, the plankton community carried by each water parcel transformed in response to nutrient injections, experiencing a succession of phytoplankton and zooplankton blooms. Eventually, various distinct water parcels were brought together by the horizontally convergent flow at E-Front. Because the water parcels were generated by different upwelling pulses (i.e., at different dates and locations along the coast), they contained plankton communities at different stages of maturity since upwelling (i.e., young parcels were dominated by phytoplankton, and older parcels dominated by zooplankton). However, because they converged at the front, they were located very close to one another in space (within the 25 km sampled by an in situ transect). Thus, the horizontal convergence of water parcels of different ages since upwelling (and thus different plankton communities) created finescale variations in the distribution of plankton abundances across the front, thus the generation of cross-frontal plankton patchiness.

The critical mechanisms underlying cross-frontal plankton patchiness have been previously discussed in other studies; however, they are often treated—and analyzed—separately. These key concepts can be summarized by the following three points: (1) a front is a mosaic of distinct water parcels brought together by convergence; (2) plankton patchiness can be explained to only a limited extent by hydrographic properties; and (3) plankton communities transform while they are advected by currents, particularly in response to nutrient injections. Below, we discuss how these ideas have been applied in previous literature and conclude that combining these concepts within a Lagrangian framework provides us with a more holistic view of physical–biological interactions at ocean fronts.

Refining our view of finescale patchiness at ocean fronts

We found that E-Front was very patchy on small spatial scales (approximately 1–5 km). The front was composed of a mosaic of water parcels contrasting in terms of biology (i.e., the plankton community), hydrography (i.e., the water-mass type derived from temperature and salinity), and history (i.e., the origin and trajectory).

Our conclusion thus extends and complements previous findings about fronts in the California Current System. For instance, Mangolte et al. (2023) demonstrated the existence of sub-frontal-scale plankton patchiness at multiple fronts in the CCE, including E-Front. Furthermore, de Verneil et al. (2019), by inferring water-mass histories from finite size Lyapunov

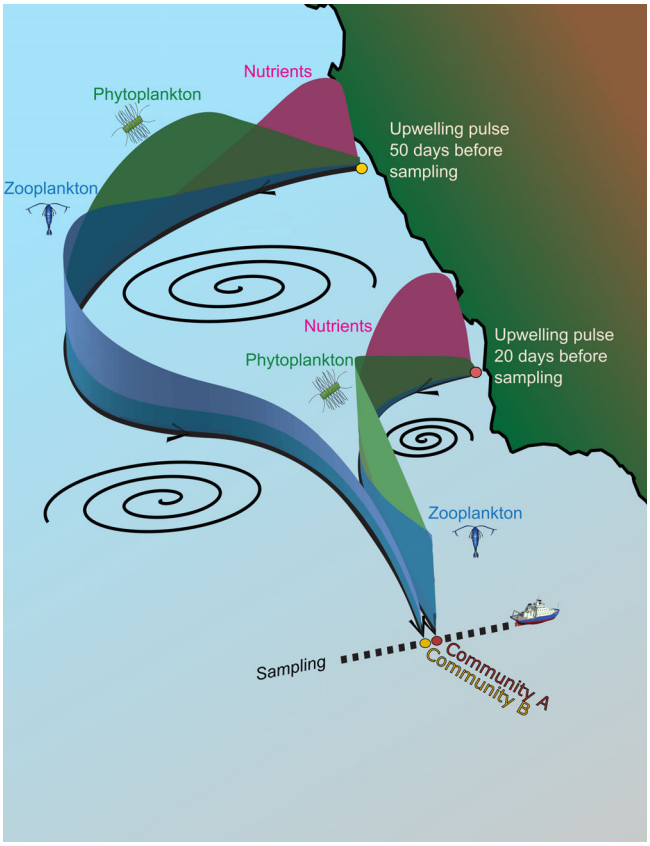

Fig. 8. Schematic representation of the biological transformation taking place in upwelled water parcels and their subsequent convergence at a front. The longer trajectory (left) originates in the north during an upwelling pulse that occurs 50 d before sampling, and the shorter trajectory (right) originates in the south during an upwelling pulse that occurs 20 d before sampling. Along each trajectory, nutrients, phytoplankton, and zooplankton concentrations peak in succession, resulting in two very different communities sampled during the cross-frontal transect. Illustration: Peter J. S. Franks and Freya Hammar. Icons: Freya Hammar (plankton) and Woods Hole Oceanographic Institution (ship).

exponents, showed that water parcels with different biological and hydrographic signatures converged at E-Front. By integrating both the approaches and data presented in Mangolte et al. (2023) and de Verneil et al. (2019) for E-Front, we have shown that cross-frontal plankton community structure was well explained by upstream and along-trajectory factors.

These results challenge the traditional representation of a front as either a well-defined, localized boundary between two distinct biogeochemical provinces (Mousing et al. 2016; Tzortzis et al. 2021), or as a homogeneous patch of enhanced productivity that emerges from a (typically) less productive background (Allen et al. 2005; Taylor et al. 2012; Mangolte et al. 2022). These views are generally associated with a focus on the local processes that control plankton community structure: in the first view, the two provinces contain different plankton communities because of the different environmental conditions (e.g., temperature, nutrients, light, etc.), while in the second view the productive patches are explained as a response to vertical processes, such as an enhanced nutrient supply or an increased exposure to light due to restratification (Mahadevan 2016; Lévy et al. 2018). In the California Current System, which already has very shallow mixed layers (Franks 2015), the restratification mechanism is unlikely to play a role. While the contribution of frontal nutrient supply is impossible to quantify without dedicated measurements, we emphasize the role of the horizontal circulation that brings together plankton communities with distinct origins, and influenced by earlier conditions. We were thus able to explain the observed plankton patchiness by invoking only upwelling dynamics and Lagrangian backtracking. It should be noted that the California Current System contains additional sources of nutrients farther offshore, mainly generated by finescale processes (such as the frontal circulation [Li et al. 2012; Kessouri et al. 2020] or eddy pumping [Gaube et al. 2013; Chenillat et al. 2015]). However, these sources appear to have influenced plankton patchiness at E-Front to a much smaller extent than horizontal transport from the coastal upwelling zone.

Integrating local hydrographic properties and Lagrangian dynamics

In a coastal upwelling system, ecosystem variability can often be explained by the variability in upwelling itself; this hinges on the idea that vertical transport of nutrient-rich waters at the coast stimulates primary production, which in turn fuels biomass of higher trophic levels (Chavez and Messié 2009; Checkley and Barth 2009). However, the pathways through which wind-driven upwelling influences the ecosystem involve both physical (particularly, horizontal currents) and biological (growth and predation) processes that are often difficult to disentangle. In this study, we attempted to explain the underlying drivers of plankton community structure using two approaches that connected a given water parcel to wind-driven coastal upwelling.

In the first approach (applying a water-mass type association), we based the connection between biology and hydrography on the following assumption: water parcels with a CU signature were likely more recently upwelled than water parcels with a CC signature, and thus CU waters likely contained higher nutrient concentrations more recently than CC waters. However, our results showed that the assumptions underlying this first approach were too simplistic, especially at very small spatial scales. For example, recently upwelled water may have acquired a CC signature by mixing with offshore waters that had recirculated inshore. Thus, we learned that we needed to understand the Lagrangian trajectories of each individual water parcel to better analyze the relationship between their hydrographic and biological signatures.

Therefore, in the second approach, we used a Lagrangian backtracking analysis to explicitly describe the upwelling conditions experienced by a given water parcel. We found that the timing and location of upwelling influenced the biological

history of each water parcel, and that qualitatively describing a water parcel as "recently upwelled" (as was the case with the first approach) was not precise enough to explain biological patterns. For example, we found that two CU water parcels may have been accurately described as "recently upwelled," but if 20 d had elapsed since upwelling for the 1st one and 50 d for the 2nd one, they would have had very different plankton communities (Fig. 8). The location and intensity of upwelling may have also affected the concentration and composition of nutrients available (Jacox et al. 2018). For example, dissolved iron supply, which exerts a bottom-up control on phytoplankton biomass, varies spatially along the coast, depending on factors such as shelf width, degree of sediment resuspension, and riverine inputs (Till et al. 2019; Forsch et al. 2023). These processes may drive some biological patchiness, which has been seen with diatoms across fronts (Brzezinski et al. 2015). Indeed, investigating the effects of initial nutrient concentrations and composition would require dedicated analyses that, while beyond the scope of this study, should receive further attention.

Overall, our results showed that in order to understand the drivers of plankton structure in a highly dynamic system, a local, hydrographic description of the water masses is not sufficient: all CU waters are not biologically equivalent, and sometimes CU water parcels can have more in common (in terms of biology) with a CC water parcel than another CU water parcel. The division of ocean basins into water masses, or biogeochemical provinces, is a powerful tool to understand large scale patterns of biodiversity (Longhurst 2006). However, at smaller spatiotemporal scales, this question is more appropriately addressed through a Lagrangian approach that describes the history of the water parcels.

The Lagrangian history: A powerful framework to understand plankton community structure

In this study, we found that the spatial structure of plankton communities is better explained by a Lagrangian metric like time since upwelling than by the hydrographic properties of the water parcel. Thus, analyzing the Lagrangian history of biological data allows for a more comprehensive view of plankton ecosystem dynamics.

Many studies, using a variety of approaches, have similarly investigated how plankton communities carried by horizontal currents transform in response to an initial nutrient injection, driven by coastal upwelling or by other processes. For instance, empirical studies have taken advantage of iron fertilization experiments to explore how phytoplankton blooms develop in response to a natural or artificial iron source (Boyd et al. 2007; Robinson et al. 2014; d'Ovidio et al. 2015), while retentive eddies give a unique glimpse into the transformation of a virtually isolated plankton community over a few weeks or even months (Lehahn et al. 2011; Chenillat et al. 2015).

Other studies have used growth-advection models—validated by in situ observations—to describe how chlorophyll and zooplankton patches are generated downstream of a nutrient source (Lehahn et al. 2017; Messié and Chavez 2017; Ser-Giacomi et al. 2023). Lagrangian approaches can also help elucidate the physical mechanisms driving phytoplankton blooms, such as nutrient injections driven by finescale turbulence (Hernández-Carrasco et al. 2023), or iron enrichment driven by interactions with islands (Della Penna et al. 2018) or seamounts (Sergi et al. 2020).

Conclusion

In this study, we employed a novel Lagrangian framework based on empirical data (in situ sampling and satellite observations) and water-parcel backtracking to demonstrate that the observed plankton patchiness across a front in the California upwelling region can be explained by distinct biological histories along converging trajectories.

This framework allows us to explicitly employ the dimension of time, thus challenging the static view of fronts and underscoring the notion that in order to identify the processes driving frontal plankton communities, we must view them as responses to their spatial and temporal histories rather than solely resulting from local frontal dynamics. For instance, the many frontal studies in the California Current System (including the present study and others referenced above) show that even superficially similar fronts located in the same region can be driven by completely different processes (e.g., nutrient injections by the frontal vertical circulation or horizontal transport from the coastal upwelling), and that more effort should be directed toward identifying these processes.

Thus, we encourage the widespread adoption of Lagrangian approaches such as satellite-based backtracking analyses, modeling studies, or dedicated in situ sampling strategies aimed at collecting data along water-parcel trajectories. The inclusion of these Lagrangian approaches will be beneficial to research efforts aimed at gaining a better understand of the mechanisms generating and maintaining biodiversity in the ocean, especially at small scales.

Data availability statement

The satellite-derived data used for our analyses and/or figures can be downloaded from the CMEMS website (https://marine.copernicus.eu/) and the Aviso + website (https://www.aviso.altimetry.fr/en/home.html). The velocity dataset is cataloged here: https://doi.org/10.48670/mds-00327. The sea-surface temperature dataset is cataloged here: https://doi.org/10.48670/moi-00169. The finite-size Lyapunov exponent (FSLE) dataset is cataloged here: https://doi.org/10.24400/527896/a01-2022.002. The P1208 cruise data are available on the CCE LTER Datazoo website (https://oceaninformatics.ucsd.edu/datazoo/catalogs/ccelter/datasets) or from the Environmental Data Initiative (searchable through the ezCatalog: https://ccelter.ucsd.edu/data/). The Coastal Upwelling Transport Index data are available here: https://mjacox.com/upwelling-indices/.

References

Allen, J. T., and others. 2005. Diatom carbon export enhanced by silicate upwelling in the northeast Atlantic. Nature **437**: 728–732. doi:10.1038/nature03948

Barth, J. A., S. D. Pierce, and R. L. Smith. 2000. A separating coastal upwelling jet at Cape Blanco, Oregon and its connection to the California Current System. Deep-Sea Res. II Topic. Stud. Oceanogr. **47**: 783–810.

Bograd, S. J., I. D. Schroeder, and M. G. Jacox. 2019. A water mass history of the Southern California current system. Geophys. Res. Lett. **46**: 6690–6698. doi:10.1029/2019GL082685

Boyd, P. W., and others. 2007. Mesoscale iron enrichment experiments 1993–2005: Synthesis and future directions. Science **315**: 612–617. doi:10.1126/science.1131669

Brzezinski, M. A., J. W. Krause, R. M. Bundy, K. A. Barbeau, P. Franks, R. Goericke, M. R. Landry, and M. R. Stukel. 2015. Enhanced silica ballasting from iron stress sustains carbon export in a frontal zone within the California Current. J. Geophys. Res. Oceans **120**: 4654–4669. doi:10.1002/2015JC010829

Chabert, P., F. D'Ovidio, V. Echevin, M. R. Stukel, and M. D. Ohman. 2021. Cross-shore flow and implications for carbon export in the California Current Ecosystem: A Lagrangian analysis. J. Geophys. Res. Oceans **126**: 1–14.

Chavez, F. P., and M. Messié. 2009. A comparison of eastern boundary upwelling ecosystems. Prog. Oceanogr. **83**: 80–96.

Checkley, D. M., and J. A. Barth. 2009. Patterns and processes in the California Current System. Prog. Oceanogr. **83**: 49–64.

Chelton, D. B., P. Gaube, M. G. Schlax, J. J. Early, and R. M. Samelson. 2011. The influence of nonlinear mesoscale eddies on near-surface oceanic chlorophyll. Science **334**: 328–332. doi:10.1126/science.1208897

Chenillat, F., P. J. Franks, P. Rivière, X. Capet, N. Grima, and B. Blanke. 2015. Plankton dynamics in a cyclonic eddy in the Southern California Current System. J. Geophys. Res. Oceans **120**: 5566–5588. doi:10.1002/2015JC010826

Clayton, S., S. Dutkiewicz, O. Jahn, and M. J. Follows. 2013. Dispersal, eddies, and the diversity of marine phytoplankton. Limnol. Oceanogr. Fluids Environ. **3**: 182–197. doi:10.1215/21573689-2373515

de Verneil, A., and P. J. Franks. 2015. A pseudo-Lagrangian method for remapping ocean biogeochemical tracer data: Calculation of net Chl-a growth rates. J. Geophys. Res. Oceans **120**: 4962–4979. doi:10.1002/2015JC010898

de Verneil, A., P. J. Franks, and M. D. Ohman. 2019. Frontogenesis and the creation of fine-scale vertical phytoplankton structure. J. Geophys. Res. Oceans **124**: 1509–1523. doi:10.1029/2018JC014645

Deibel, D., and B. Lowen. 2012. A review of the life cycles and life-history adaptations of pelagic tunicates to environmental conditions. ICES J. Mar. Sci. **69**: 358–369. doi:10.1093/icesjms/fsr159

Della Penna, A., T. W. Trull, S. Wotherspoon, S. De Monte, C. R. Johnson, and F. D'Ovidio. 2018. Mesoscale variability of conditions favoring an iron-induced diatom bloom downstream of the Kerguelen Plateau. J. Geophys. Res. Oceans **123**: 3355–3367. doi:10.1029/2018JC013884

d'Ovidio, F., V. Fernández, E. Hernández-García, and C. López. 2004. Mixing structures in the Mediterranean Sea from finite-size Lyapunov exponents. Geophys. Res. Lett. **31**: 1–4.

d'Ovidio, F., S. De Monte, S. Alvain, Y. Dandonneau, and M. Lévy. 2010. Fluid dynamical niches of phytoplankton types. Proc. Natl. Acad. Sci. USA **107**: 18366–18370. doi:10.1073/pnas.1004620107

d'Ovidio, F., and others. 2015. The biogeochemical structuring role of horizontal stirring: Lagrangian perspectives on iron delivery downstream of the Kerguelen Plateau. Biogeosciences **12**: 5567–5581. doi:10.5194/bg-12-5567-2015

Dugenne, M., F. Henderikx Freitas, S. T. Wilson, D. M. Karl, and A. E. White. 2020. Life and death of *Crocosphaera* sp. in the Pacific Ocean: Fine scale predator–prey dynamics. Limnol. Oceanogr. **65**: 2603–2617. doi:10.1002/lno.11473

Eiane, K., and M. D. Ohman. 2004. Stage-specific mortality of *Calanus finmarchicus*, *Pseudocalanus elongatus* and *Oithona similis* on Fladen Ground, North Sea, during a spring bloom. Mar. Ecol. Prog. Ser. **268**: 183–193.

Forsch, K. O., K. C. Fulton, M. M. Weiss, J. W. Krause, M. R. Stukel, and K. A. Barbeau. 2023. Iron limitation and biogeochemical effects in Southern California Current coastal upwelling filaments. J. Geophys. Res. Oceans **128**: e2023JC019961. doi:10.1029/2023JC019961

Franks, P. J. 2015. Has Sverdrup's critical depth hypothesis been tested? Mixed layers vs. turbulent layers. ICES J. Mar. Sci. **72**: 1897–1907. doi:10.1093/icesjms/fsu175

Gangrade, S., and P. J. Franks. 2023. Phytoplankton patches at oceanic fronts are linked to coastal upwelling pulses: Observations and implications in the California Current System. J. Geophys. Res. Oceans **128**: 1–27.

Gaube, P., D. B. Chelton, P. G. Strutton, and M. J. Behrenfeld. 2013. Satellite observations of chlorophyll, phytoplankton biomass, and Ekman pumping in nonlinear mesoscale eddies. J. Geophys. Res. Oceans **118**: 6349–6370. doi:10.1002/2013JC009027

Goericke, R., and J. P. Montoya. 1998. Estimating the contribution of microalgal taxa to chlorophyll *a* in the field—variations of pigment ratios under nutrient- and light-limited growth. Mar. Ecol. Prog. Ser. **169**: 97–112. doi:10.3354/meps169097

Haberlin, D., R. Raine, R. McAllen, and T. K. Doyle. 2019. Distinct gelatinous zooplankton communities across a dynamic shelf sea. Limnol. Oceanogr. **64**: 1802–1818. doi:10.1002/lno.11152

Hernández-Carrasco, I., V. Rossi, G. Navarro, A. Turiel, A. Bracco, and A. Orfila. 2023. Flow structures with high Lagrangian coherence rate promote diatom blooms in oligotrophic waters. Geophys. Res. Lett. **50**: 1–12.

Huyer, A. 1983. Coastal upwelling in the California current system. Prog. Oceanogr. **12**: 259–284. doi:10.1016/0079-6611(83)90010-1

Jacox, M. G., C. A. Edwards, E. L. Hazen, and S. J. Bograd. 2018. Coastal upwelling revisited: Ekman, Bakun, and improved upwelling indices for the U.S. west coast. J. Geophys. Res. Oceans **123**: 7332–7350. doi:10.1029/2018JC014187

Jönsson, B. F., and J. R. Watson. 2016. The timescales of global surface-ocean connectivity. Nat. Commun. **7**: 1–6.

Kessouri, F., D. Bianchi, L. Renault, J. C. McWilliams, H. Frenzel, and C. A. Deutsch. 2020. Submesoscale currents modulate the seasonal cycle of nutrients and productivity in the California Current System. Global Biogeochem. Cycles **34**: 1–15.

Lehahn, Y., F. D'Ovidio, and I. Koren. 2018. A satellite-based Lagrangian view on phytoplankton dynamics. Ann. Rev. Mar. Sci. **10**: 99–119.

Lehahn, Y., F. D'Ovidio, M. Lévy, Y. Amitai, and E. Heifetz. 2011. Long range transport of a quasi isolated chlorophyll patch by an Agulhas ring. Geophys. Res. Lett. **38**: 1–6.

Lehahn, Y., I. Koren, S. Sharoni, F. D'Ovidio, A. Vardi, and E. Boss. 2017. Dispersion/dilution enhances phytoplankton blooms in low-nutrient waters. Nat. Commun. **8**: 1–8.

Levin, S., and L. Segel. 1976. Hypothesis for origin of planktonic patchiness. Nature **259**: 659. doi:10.1038/259659a0

Lévy, M., P. J. Franks, and K. S. Smith. 2018. The role of submesoscale currents in structuring marine ecosystems. Nat. Commun. **9**: 4758.

Lewandowska, A. M., M. Striebel, U. Feudel, H. Hillebrand, and U. Sommer. 2015. The importance of phytoplankton trait variability in spring bloom formation. ICES J. Mar. Sci. **72**: 1908–1915. doi:10.1093/icesjms/fsv059

Li, Q. P., P. J. Franks, M. D. Ohman, and M. R. Landry. 2012. Enhanced nitrate fluxes and biological processes at a frontal zone in the southern California current system. J. Plankton Res. **34**: 790–801. doi:10.1093/plankt/fbs006

Longhurst, A. R. 2006. Ecological geography of the sea, 2nd ed. Elsevier.

Lynn, R. J., and J. J. Simpson. 1987. The California Current System: The seasonal variability of its physical characteristics. J. Geophys. Res. Oceans **92**: 12947–12966. doi:10.1029/JC092iC12p12947

Mahadevan, A. 2016. The impact of submesoscale physics on primary productivity of plankton. Ann. Rev. Mar. Sci. **8**: 161–184. doi:10.1146/annurev-marine-010814-015912

Mangolte, I., M. Lévy, S. Dutkiewicz, S. Clayton, and O. Jahn. 2022. Plankton community response to fronts: Winners and losers. J. Plankton Res. **44**: 241–258. doi:10.1093/plankt/fbac010

Mangolte, I., M. Lévy, C. Haëck, and M. D. Ohman. 2023. Sub-frontal niches of plankton communities driven by transport and trophic interactions at ocean fronts. Biogeosciences **20**: 3273–3299. doi:10.5194/bg-20-3273-2023

Martin, A. 2003. Phytoplankton patchiness: The role of lateral stirring and mixing. Prog. Oceanogr. **57**: 125–174. doi:10.1016/S0079-6611(03)00085-5

McGillicuddy, D. J., and P. J. Franks. 2019. Models of plankton patchiness, p. 536–546. *In* Encyclopedia of ocean sciences, v. **1–5**, 3rd ed. Elsevier.

McWilliams, J. C. 2016. Submesoscale currents in the ocean. Proc. R. Soc. A Math. Phys. Eng. Sci. **472**: 20160117.

Messié, M., and F. P. Chavez. 2017. Nutrient supply, surface currents, and plankton dynamics predict zooplankton hotspots in coastal upwelling systems. Geophys. Res. Lett. **44**: 8979–8986. doi:10.1002/2017GL074322

Messié, M., D. A. Sancho-Gallegos, J. Fiechter, J. A. Santora, and F. P. Chavez. 2022. Satellite-based Lagrangian model reveals how upwelling and oceanic circulation shape krill hotspots in the California Current System. Front. Mar. Sci. **9**: 1–19.

Messié, M., and others. 2023. Coastal upwelling drives ecosystem temporal variability from the surface to the abyssal seafloor. Proc. Natl. Acad. Sci. USA **120**: e2214567120. doi:10.1073/pnas.2214567120

Mousing, E. A., K. Richardson, J. Bendtsen, I. Cetinić, and M. J. Perry. 2016. Evidence of small-scale spatial structuring of phytoplankton alpha- and beta-diversity in the open ocean. J. Ecol. **104**: 1682–1695. doi:10.1111/1365-2745.12634

Ohman, M. D., J. R. Powell, M. Picheral, and D. W. Jensen. 2012. Mesozooplankton and particulate matter responses to a deep-water frontal system in the southern California Current System. J. Plankton Res. **34**: 815–827. doi:10.1093/plankt/fbs028

Rio, M. H., S. Mulet, and N. Picot. 2014. Beyond GOCE for the ocean circulation estimate: Synergetic use of altimetry, gravimetry, and in situ data provides new insight into geostrophic and Ekman currents. Geophys. Res. Lett. **41**: 8918–8925. doi:10.1002/2014GL061773

Robinson, J., E. E. Popova, A. Yool, M. Srokosz, R. S. Lampitt, and J. R. Blundell. 2014. How deep is deep enough? Ocean iron fertilization and carbon sequestration in the Southern Ocean. Geophys. Res. Lett. **41**: 2489–2495. doi:10.1002/2013GL058799

Rossi, V., V. Garçon, J. Tassel, J. B. Romagnan, L. Stemmann, F. Jourdin, P. Morin, and Y. Morel. 2013. Cross-shelf variability in the Iberian Peninsula Upwelling System: Impact of a mesoscale filament. Cont. Shelf Res. **59**: 97–114. doi:10.1016/j.csr.2013.04.008

Rossi, V., E. Ser-Giacomi, C. Lõpez, and E. Hernández-García. 2014. Hydrodynamic provinces and oceanic connectivity from a transport network help designing marine reserves. Geophys. Res. Lett. **41**: 2883–2891. doi:10.1002/2014GL059540

Sarthou, G., K. R. Timmermans, S. Blain, and P. Tréguer. 2005. Growth physiology and fate of diatoms in the ocean: A review. J. Sea Res. **53**: 25–42. doi:10.1016/j.seares.2004.01.007

Schmid, M. S., S. Sponaugle, A. W. Thompson, K. R. Sutherland, and R. K. Cowen. 2023. Drivers of plankton community structure in intermittent and continuous coastal upwelling systems—from microbes and microscale in-situ imaging to large scale patterns. Front. Mar. Sci. **10**: 1–22.

Sergi, S., A. Baudena, C. Cotté, M. Ardyna, S. Blain, and F. D'Ovidio. 2020. Interaction of the Antarctic Circumpolar Current with seamounts fuels moderate blooms but vast foraging grounds for multiple marine predators. Front. Mar. Sci. **7**: 1–18.

Ser-Giacomi, E., R. Martinez-Garcia, S. Dutkiewicz, and M. J. Follows. 2023. A Lagrangian model for drifting ecosystems reveals heterogeneity-driven enhancement of marine plankton blooms. Nat. Commun. **14**: 6092.

Stukel, M. R., and others. 2017. Mesoscale ocean fronts enhance carbon export due to gravitational sinking and subduction. Proc. Natl. Acad. Sci. USA **114**: 1252–1257.

Stukel, M. R., M. D. Ohman, C. R. Benitez-Nelson, and M. R. Landry. 2013. Contributions of mesozooplankton to vertical carbon export in a coastal upwelling system. Mar. Ecol. Prog. Ser. **491**: 47–65. doi:10.3354/meps10453

Taylor, A. G., R. Goericke, M. R. Landry, K. E. Selph, D. A. Wick, and M. J. Roadman. 2012. Sharp gradients in phytoplankton community structure across a frontal zone in the California Current Ecosystem. J. Plankton Res. **34**: 778–789. doi:10.1093/plankt/fbs036

Till, C. P., J. R. Solomon, N. R. Cohen, R. H. Lampe, A. Marchetti, T. H. Coale, and K. W. Bruland. 2019. The iron limitation mosaic in the California Current System: Factors governing Fe availability in the shelf/near-shelf region. Limnol. Oceanogr. **64**: 109–123. doi:10.1002/lno.11022

Tzortzis, R., and others. 2021. Impact of moderately energetic fine-scale dynamics on the phytoplankton community structure in the western Mediterranean Sea. Biogeosciences **18**: 6455–6477. doi:10.5194/bg-18-6455-2021

Wilkins, D., E. Van Sebille, S. R. Rintoul, F. M. Lauro, and R. Cavicchioli. 2013. Advection shapes Southern Ocean microbial assemblages independent of distance and environment effects. Nat. Commun. **4**: 2457.

Zaba, K. D., D. L. Rudnick, B. D. Cornuelle, G. Gopalakrishnan, and M. R. Mazloff. 2018. Annual and interannual variability in the California current system: Comparison of an ocean state estimate with a network of underwater gliders. J. Phys. Oceanogr. **48**: 2965–2988. doi:10.1175/JPO-D-18-0037.1

Zaba, K. D., P. J. S. Franks, and M. D. Ohman. 2021. The California Undercurrent as a source of upwelled waters in a coastal filament. J. Geophys. Res. Oceans **126**: 13. doi:10.1029/2020JC016602

Acknowledgments

The authors would like to warmly thank Peter J. S. Franks, Marina Lévy, Mark Ohman, Ralf Goericke, Pierre Chabert, Katherine Zaba, and Michael Stukel for providing data, guidance, and/or feedback. The authors are also grateful to Peter J. S. Franks (schematic) and Freya Hammar (schematic and icons) for their illustrations, and the ship/science crews on the *R/V Melville* in August 2012. SG was funded by the NSF GRFP and Scripps Institution of Oceanography. IM was funded by an ENS/Sorbonne Université PhD grant, a Fulbright Scholarship, and CNES. Support for CCE LTER was provided by NSF OCE-1637632/OCE-1026607/OCE-2224726.

Conflict of Interest

The authors declare no conflict of interest.

Submitted 10 April 2024
Revised 21 June 2024
Accepted 23 July 2024

Associate editor: David Antoine